Synthesis of ultra-thin membrane layers by plasma treatment of Langmuir-B[odgett and self-assembly film:

Brite-EuRam Project no. 7536
CEC Contract no. BRE2-CT93-0572

Synthesis Repofi

Reporting period: 01.01.94-31.03.96

NON-CONFIDENTIAL

Coordinator:
P. Detemple, V. Hessel ~
[MM Institute of Microtechnology Mainz GmbH, **Mainz, Germany**

Partners:
R. Terpstra
CTK Centre for Technical Ceramics, **Eindhoven, Netherlands**
O N. Kannellopo]ous
DEMOCRfTOS Centre for Scientific Research, **Athens, Greece**

Endorsers:
AKZO Central Research, **Obernburg, Germany**
DEUTSCHE CARBONE AG, **Neunkirchen-Heiniti, Germany**
SCT Societe des Ceramiques Techniques, **Bazet, France**
VELTEROP Ceramic Membrane Technology, **Enschede, The Netherlands**
FOCO LTD - Solar Energy, **Athens, Greece**

Mainz, November 1996

IMM Institut fur Mikrotechnik Mainz GmbH
D-551 29 Mainz-Hechfsheim, Carl-Zeiss-StraRe 18-20, German y

Table of contents

1. Abstract

Main scientific aim of this focused fundamental research project has been the investigation of the interaction of low temperature plasmas with metal-organic Langmuir-Blodgett-films in order to create ultra thin, defect-free ceramic-like structures by controlled conversion of organic film. The applied aspect of the work under the project was directed to the preparation and investigation of model membranes using a metal oxide ceramic-like separation layer created by the technique described **above and fixed on a microporous ceramic substrate.**

The processing of the ceramic substrates was carried out either by s6ip casting (flat substrates) or paste processing (hollow fibre substrates). Flat membranes were produced from silicon nitride, hollow fibre membranes from aluminium oxide and silicon nitride. Slip casting was performed using a colloidal stabilised aqueous suspension of the ceramic powders. The process allows the variation of the median pore size from O (dense) to 0.65 micrometer using different amounts of sintering aids. Paste processing was carried out for the preparation of the hollow fibre ernbranes using a polymeric body in which the ceramic powders are dispersed up w o a high volume content. The fibre obtained characteristics are: diameter down to t mm, wa!l thickness down to 100 pm, membrane surface to volume ratio over 1000 m 2 / m 3 .

For the preparation of the selective layer an Mgz^{+}- stearic acid system was chosen. The subphase was made basic to guarantee full complexatiog of the amphiphile in order to achieve a ratio of inorganic to organic material as high as possible. With this system were on silicon substrates perfect transfer conditions for single and multilayers were obtained. By subsequent exposition of the film to a low temperature oxygen or argon plasma the organic part of the transferred mu{tilayer structure was decomposed leaving an ultra thin film. AFM-investigations showed, that the resu!ting films have a uniform grainy structure, but exhibit a small number of long cracks probably due to shrinkage of the film during plasma treatment. H was also shown, that the remaining organic material in the multilayers can be minimised by variation of the plasma process parameters.

While the transfer of the LB-multi\ ayers on flat non porous substrates worked very ~11, the LB-coating of the micro porous substrates turned out to be **the most serious problem [n the project. In order to solve this problem a iarge number of different processes for the creation of an appropriate interface iayer were tested such as l_ow Pressure Chemical Vapour Deposition (LPCVD) and Physical Enhanced Chemical Vapour Deposition (PECVD) of s'ilicon oxide and silicon nitride, or plasma deposition amorphous hydrocarbon films. Good transfer conditions for the L8-multilayer system were at /east obtained by the application ,of a ~-aluminium oxide interface layer exhibiting a very smooth surface and a pore size in the nm range. However also in this case only poor gas selectivities were obtained.**

furnace (KCE, Germany). A heating rate of 10°C/min is used. The silicon nitride is sintered in a Nz atmosphere at 100 kPa pressure. Samples are embedded in a powder bed (prepared from silicon nitride (SN-EI O, UBE) and Boron Nitridepowder) in a Silicon Carbide crucible when sintdred. All samples are sintered at 1600°C (pyrometer controlled) with a heating and cooling rate of 10°C/min.

3.1.3. Properties of fabricated substrates

The porosity of the silicon nitride materials can be as high as 50 '/0, when no sirttering aid is used at aJL The properties of the silicon nitride material are shown in the following graphs and tables.

Figures 1 and 2 show the pore size and pore size distribution (obtained by Hg-porosimetry) for two batches of flat silicon nitride substrates containing O respectively 20 '/o of sintering aid. Per batch the distribution is quite reproducible. The pore size initially increases with increasing amount of sintering aid. Above & 10 0/~ of sintering aid, it decreases. The porosity decreases with increasing amount of sintering aid, as can be expected. It is found that by increasing the amount of. sistering additive, the rosity decreases as expected, however, the pore size increases, reaches a m ximum around 5 % and decreases. These results were confirmed. It was decided to repeat the experiment with more samples.

It seems that the addition of a limited amount of sinter additive enhances the densification of domains or agglomerates. No macroscopic densification occurs as can be seen from the table. It seems likely that around agglomerates large pores are formed. The mean pore size increases, distribution broadens. With increasing sinter additive domains start “to ,see” (percolation) each other, and macroscopic densification takes place now as can be seen from the table. The volume fraction of large pores decreases as well as the” pore size and the pore size distribution becomes smaller.

Extrapolation of the strength values from the table to zero porosity, using the model proposed by Ryskewitsch (J. Amer Cer&m. Sot., 36, 65 (1953)) gives a value of 1540 MPa, which seems quite realistic.

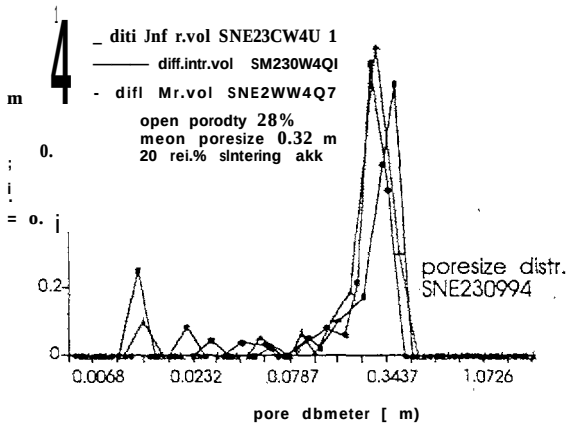

Fig. 1. Pore size distribution for sintered SNE-10 silicon nitride compact containing 207. of sintering aid.

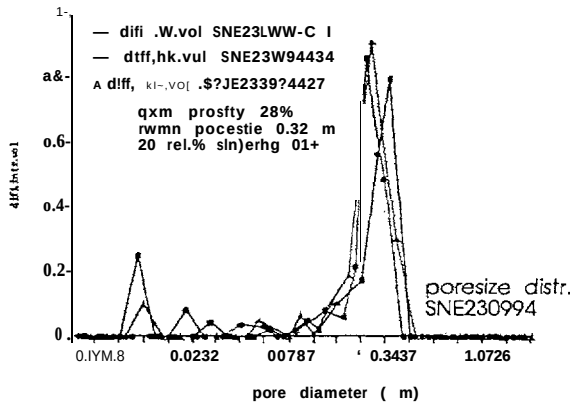

Fig. 2. Pore size distribution of sintered SNE-I O compact without sintering aid.

The pore size distribution of all samples is rather broad. By increasing the amount of sintering aid, the pore size typically increases to 0.7-0.8 pm and then ,shows a sharp

decrease, as shown in figure 3. This phenomenon is possibly related to an inhomogeneous distribution of the sintering aid in the compact. As stated before further research to understand this phenomenon will be carried out. It looks an interesting tool because it seems to be possible to change the pore size dramatically with only small changes in the amount of additive, while the porosity remains relatively high (up to 35 Yo). The pore size distribution however broadens with increasing pore size, which can be disadvantages.

The micro structure of sintered SNE-1 O silicon nitride compacts with increasing concentration of sintering aid. There is a good qualitative agreement with the data in figure 3.

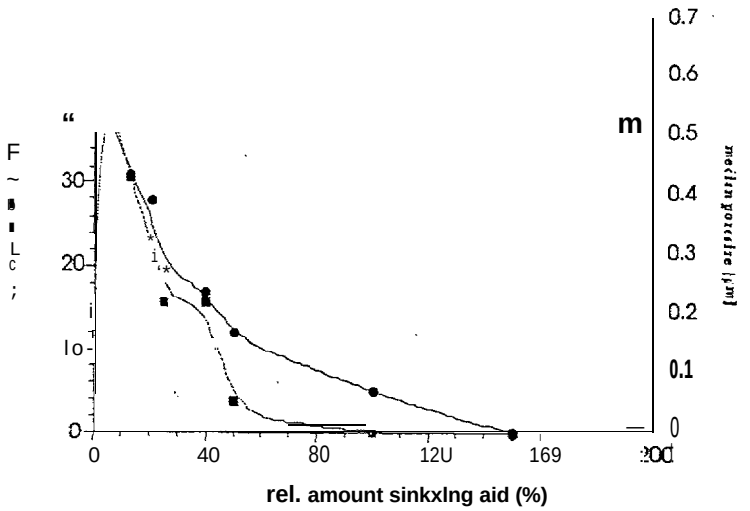

Figure 3. Open porosity and median poresize versus amount of sintering aid used.

3.2. Preparation of the selective layer by LB=film deposition and subsequent plasma treatment

3.2.1. Low temperature dasma treatment of the LB-multilavers

series of samples was treated by low temperature-plasma with the aim to convert e mixed organic-inorganic ultrathin film to a ceramic-like inorganic material avoiding nonuniform agglomerisation and formation of new defects.

Oxygen and argon were chosen as process gases, the gas flow rate and the pressure were kept constant, the radio frequency (RF) power and the exposure time were varied. ~

3.2.2. Determination of the LB-multilaver structure by X-rav measurements before and after ~lasma treatment

The diffraction patterns of the LB films show a large number of Bragg peaks as well as of Kiessig fringes 1 I ,14. information on the thickness and the quality of the fi~m can be derived from an analysis of the Kiessig fringes. Even at wide angles a large number of Kiessig fringes are observed. This confirmes that the film is uniform and that the surface is smooth. The toial film thickness calculated from the distance between the Kiessig fringes amounts to 422 ~. By dividing this value by the number of dipping cycles (eight), a value of 52.7 ~ per layer is obtained. The internal structure of the LB-mu[tilayer is obtained from the analysis of the Bragg peaks. 12

pronounced Bragg peaks are detected for scattering angles (2$) ranging between 0.5° and 30°. Accordingly, the internal order has to be very high and the multilayer system is well defined. The Bragg peaks can be related to a periodic bilayer structure and can be indexed up to the 15th order. A d-spacing of 52.3 ~ results.

After plasma treatment the X-ray diffraction patterns clearly show a reduced number of Bragg peaks, whilst Kiessig fringes can no longer be detected. The intensity of the single peaks is likewise reduced. .The absence of the Kiessig fringes was expected, because the surface roughness of the plasma treated samples was significantly higher than those of the LB-films. Comparing samples treated at the lowest RF-power (5 W) with those treated at higher RF-power (15 up to 50 W), it can be seen that both the number and intensity of the Bragg peaks decreases with increasing RF-power of the plasma. This is due to the progressive destruction of the multilayer. On the other hand this diffraction pattern clearly shows that there is still an internal order in the film even if treated with 30 W RF-power.

3.2.3. Determination of the chemical composition of the LB-multilayers bv FTIR measurements before and after dasma treatment

@ The C=O stretching mode of the carboxylic acid group 15 which is usually located at 1695 and 1705 cm-l is missing in the spectrum of the Mg-stearate multilayers. Instead, a strong band is observed at 1561 cm-l which has been assigned to the asymmetric [Va(C02)] stretching vibration of the $C0_2$-anion of the fatty acid salt 1 s,~ 6 and proves that the content of noncomplexed stearic acid molecules can be assumed to be very small (< 10/O). This clearly shows that the monolayer is transferred from the film balance to the substrate as magnesium stearate and not as free acid. The broad band with two maxima at 34!52 and 3332 cm-l can be assigned to the OH vibration of hydrated water within the metal ion layer.

After plasma treatment at low RF-power (5 W) and with short exposure time (50 s) still the same bands with a similar relative ratio as for the untreated sample are found, but the total absorbance is decreased by a factor of nearly two. More intense plasma treatment (higher RF-power and/or higher exposure time: up to 50 W and 300 s) leads to a more pronounced decrease of the total intensity and to a disappearance or broadening of the asymmetric [va(C=O)] stretching vibration of the

@ cu~-anion. The asymmetric [v~(CH,)] and the two CHZ stretching vibrations are still unchanged, while the [5(CH_2)] bending and the hydrated water vibrations disappear 15,16

A similar infiuence of the argon plasma treatment on the FTIR spectra was found: The appearance of new bands in the FTIR-spectra for both oxygen and argon treated samples were not found. Hence, no new functional groups have been introduced as reported before for cadmium-arachidate and polysiloxane multilayers Z4JPS. This difference is probably a consequence of the use of a radiofrequency instead of a microwave plasma 12,13, the latter of which exhibits enhanced etching and ablation rates. {n addition, pure reorientation effects (without any ablation or etching) are not observed lz~ls.

Since a small absorbance due to the stretching [v(CHz)] vibrations was detected even for the sample treated at 50 W, a small amount of organic material still remains. Successive thermal treatment will be used for further removal of this residual organic part. Yet, the plasma treated films should be described as organo-ceramic materials instead being truly inorganic.

A semi-quantitative analysis of the decomposition of the organic material was performed by plotting the peak area of the strong Cf-f~ and CH_2 stretching vibrations as a function of the W-power or the exposure time (see figure 4). A steep decrease in the peak area with more intense plasma treatment is found. This confirms that the application of plasma even at a comparatively low dose has a significant influence on the organic material.

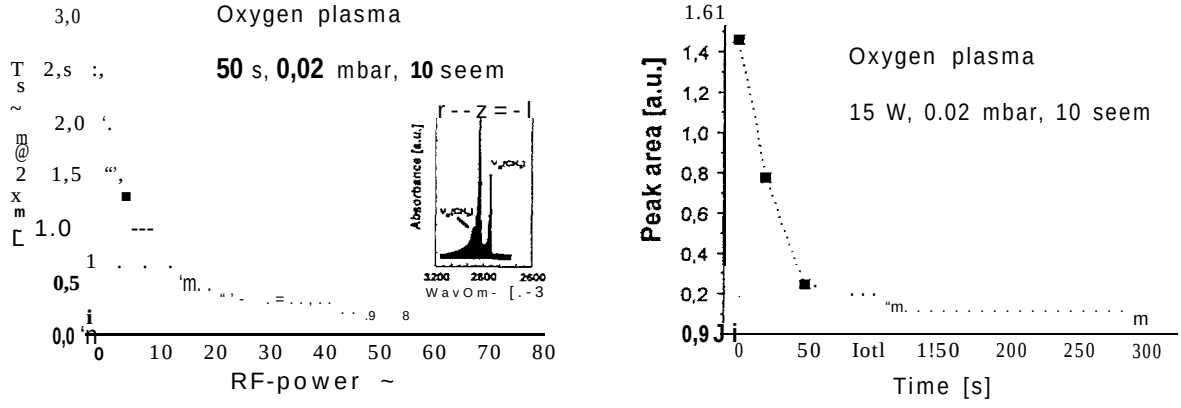

Fig. 4: Peak area versus W-power diagram (18 oxygen plasma treated multilayers)
Peak area versus time diagram (18 oxygen plasma treated multi layers).

3;2.4. Determination of the surface topography of the U3-multilavers by AFM-rneasurements before and after plasma treatment ,

The AFM experiments of 16 Mg-stearate multilayers show two types of images (5pm * 5 pm): In some images homogeneous smooth layers are found, whilst others j display large domains of different height (see figures 5a and b).

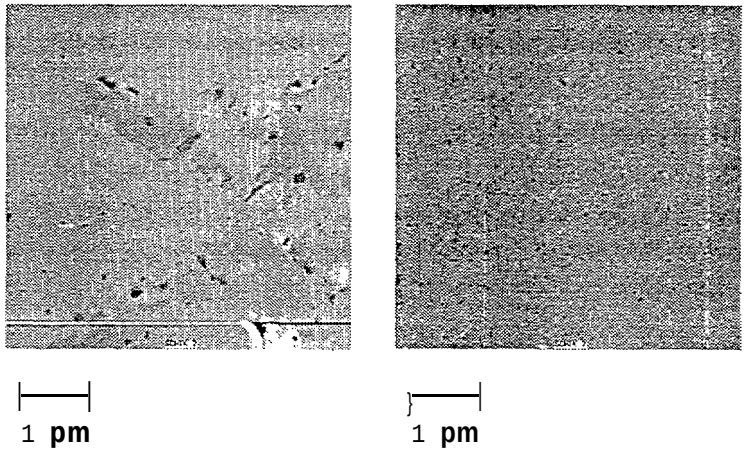

Figure 5: AFM-image of 16 magnesium stearate multilayers on a Si-support.
a) 5 pm * 5vrn AFM-image with domains of different height and both large and small pinholes
b) **5** pm * **5pm AFM-image with homogeneous surface and small pinholes**

Measurements at different locations on one substrate or on different substrates show that both types of images are distributed with similar frequency. Since during the LB-transfer the deposited area increases for the first three monolayer and then reaches an approximately constant value, it is very likely that this incomplete transfer causes the formation of these domains. Thus, the height of the domains should be

comparable to the length of one bilayer and this is, in fact, found when the' height-profile of the AFM-image is analyzed. Furthermore, a considerable number of pinholes are found in both figures 5a and b which presents a significant drawback if these films would be used for gas separation without any plasma treatment. An AFM-image of 38 rnultilayers shows an even more pronounced domain structure. Since at most 3 to 4 steps are found, it is evident that the domain structure is a consequence of incomplete transfer at the very .begirming and that subsequent layers are regulariy deposited. In addition, almost complete absence of deep pinholes is observed, thereby indicating a cioser coverage with increasing number of iayers although the surface is not perfectly smooth.

A 5 pm * 5 j.un AFM-image of a sampie treated with a 5 W-oxygen piasma is stiii similar to the image of the untreated sample (see figures 5 and 6). Domains with different numbers of deposited multilayers create a steplike height profiie of the surface and furthermore pinhoies are present.

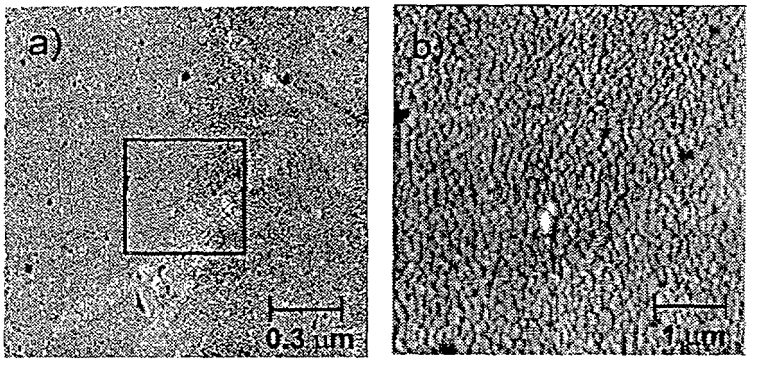

Figure 6: AFM images of 18 oxygen plasma treated magnesium stearate multilayers orl a Si-supporl (5 W, !50 s, 10 seem, 0.02 mbar)

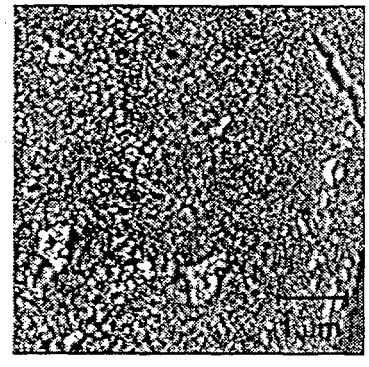

Figure 7:4 ~m * 4 ~m AFM-image of 18 oxygen plasma treated magnesium stearate multilayers on a Si-support (50 W, 50 s, 10 seem, 0.02 mbar)

Nevertheless, a grainy substructure can be observed inside these domains which is not found for untreated samples and which is probably caused by etching processes. The 1.5 ~m * 1.5 ~m magnification of a part of this image shows even more ciearly that the surface roughness increases after plasma treatment.

A 4 p.m * 4 ~m AFM-image of a sample treated with 50 W-oxygen piasma shows a grainy surface structure without any similarity to the original multilayer structure (see figure 7). Deep pinholes are no longer present, but some images show cracks in the ym range which are probably due to different thermal expansion coefficients and densities of organic and inorganic materiai. Nevertheiess, apart from the existence of these cracks the Si-surface is stiii completely covered after the piasma treatment: No smooth areas of the underlying substrate as well as isoiated crystals or iarger moiten dropiets are found. Ali in aii, the surface profiie is more homogeneous after plasma treatment than before. These results are quite different to those obtained uuring thermal decomposition of LB-muitilayers 9110.

3.3. **Evaluation of the membrane properties**

3.3.1. Investigated types of membranes

Three different types of membranes have been prepared by deposition of thin films on supports. They differ in the morphology of the undedying support ("dense" or porous) and in the geometry (flat or cylindrical).

- **Flat supported porous membranes**
- **Flat composite membranes**
- **Hollow fibre composite membranes**

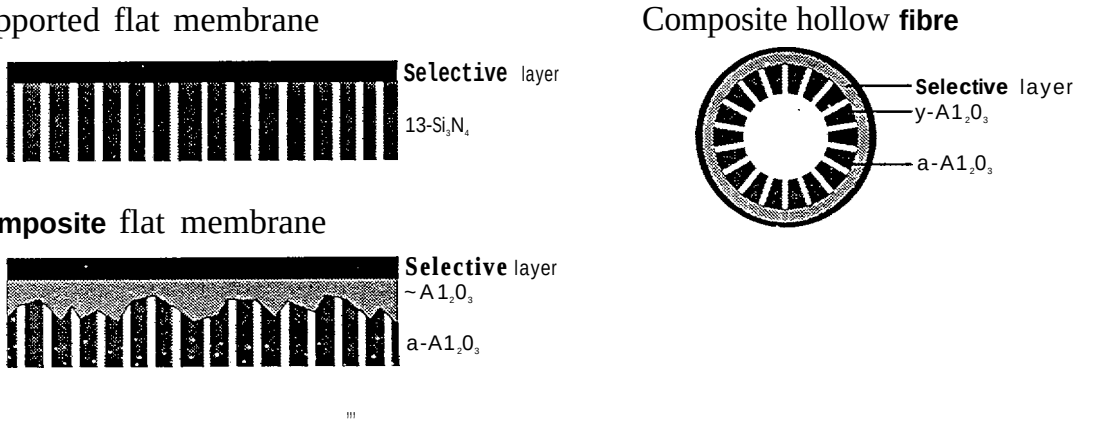

Scheme 2: Investigated types of membranes

The *supporfea' membranes* are built of" two components, namely the underling support and !he selective layer on top of it.
The *composite membranes* are three-component systems with a support, intermediate layer and thin selective layer. In addition to the porous support, the composite membranes contain an intermediate layer with very small pores <3 nm. The intermediate layer will either be dominantly selective, if the permeability is lower than that of the support. It will enhance the selectivity of the support, if the permeability is higher than that of the support.
At the begi;ning,"flat geometries were preferred due to the easier deposition of films and the availability of a number of techniques allowing a determination of permeation properties. It was intended to extend the concepts from flat geometries to cylindrical ones (hollow 'fibres). The latter ones are more suitable for industrial applications, since they have a higher active surface to volume ratio.

3.3.2. The components of the membranes

The support
As supports sintered porous ceramic "materials were used. For membranes *without* intermediate layer &Si_3N_4 disks we're used (3.0 cm diameter, 2 mm thickness). The open porosity was varied from 48 to 28 and 17°/0 by adding different amounts of the sintering aid ($A1_20_3$, Y_20_3). The average pore size was 200 nm. For membranes with intermediate layer U-$A1_20_3$ disks were used (3.9 cm diameter, 2 mm thickness,

Velterop company). The open porosity was approximately 50%. The average pore size was 150 nm.

The intermediate [aver

The intermediate layer (Velterop company) was a y-$A1_20_3$ film prepared by sol-gel-technique from A1-tri(kopropylate). The main pore size was 3 nm. In contrast to the supports, the pore sizes of the intermediate layer are not symmetrically, distributed to ~ larger and smaller values. There is only a samll, number of pores of larger size (cut-off at 3 rim).

The selective lavers

Selective layers have been deposited by several thin film techniques, namely LB (Langmuir-Blodgett) technique, LPCVD (Low pressure chemical vapour deposition), PECVD (Plasma enhanced chemical vapour deposition), plasrnapolymerization, sputtering and evaporation. In some cases thermal follow-up treatment is necessary to improve the properties of the layer, namely plasmatreatment and thermodesorption or pyrolysis. in both cases the major function of the follow-up treatment is the removal of the organic content.

3.3.3. Gas separation measurements of LB-coated membranes

A characteristic feature of all measured LB-coated membranes are the relatively high reduced permeabilities of the four gases hydrogen, nitrogen, carbon dioxide and butane (see figure 8). The perry eabilities found were even in the order of those of the . uncoated membranes.

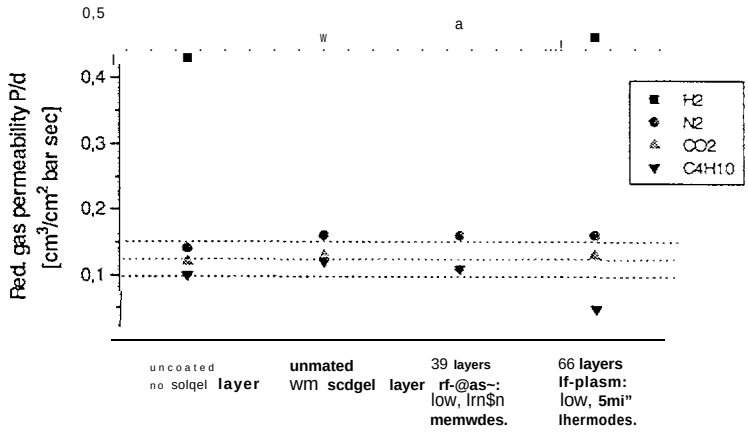

Fig. 8: Reduced permeability of hydrogen, nitrogen, carbon dioxide and butane for uncoated and LB-coated membranes with intermediate layers.

The permeability of one gas is nearly constant for different types of LB membranes, thus, it seems to be independent of most mportant process parameters.

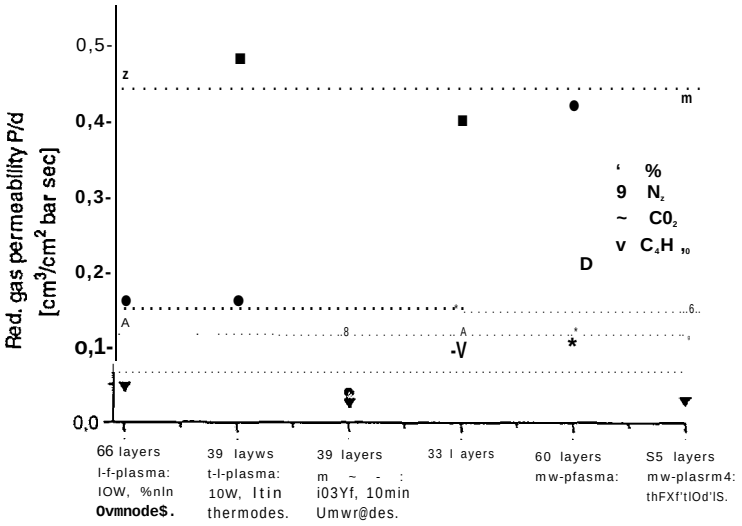

Fig. 9: Reduced gas permeabilities of six different LB-coated composite membranes.

In particular, there is obviously no dependence on the LB-transfer (e.g. number of monolayer), plasma treatment (e.g. type pf plasma: MW + RF), power input, time of exposure and thermodesorption.
The ideal selectivity was calculated by dividing the permeability of hydrogen by those the other gases. The so determined selectivities of the i_ B-membranes were relatively low for most gases (see figure 1 O).

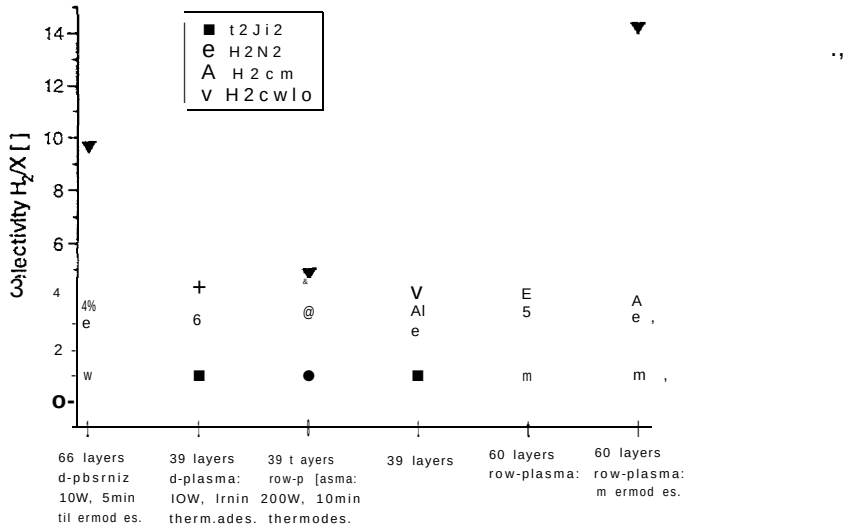

Fig. 10: Idea[selectivities of hydrogenlhydrogefl, hydrogenhitrogen, hydrogen/carbon dioxide and hydrogen}butane for six different LB-coated composite membranes.

However, there were two exceptions which showed enhanced selectivities for butane/hydrogen. All olher values are in the order of the Knudsen ratio. Thus, a separation based on molecuiar weight of the gases is most iikely to occur. The partially considerable deviations of the measured values from the Knudsen ratio may

be a result of surface diffusion terms. There is rto hjni for an extraordinary increase. in selectivity which can be referred to the presence of molecular sieving.
A correlation of the permeabilities and selectivities measured to the process parameters of the preparation - namely LB technique, plasma treatment and thermo-desorption - is hardly possible on the basis of the present data. There is even no general difference for samples where one or two of the process steps have been omitted (see the last three samples in figure 10).
To summarize, the motivation for an investigation of LB-membranes was mainly guided by two expectations: Due to their low thickness high permeabilities should result, the absence of defects should lead to moderate to high selectivities. Although high permeabilities are proven by the experimental data, it is astonishing that no additional (small) resistance is found as a result of LB-deposition. The relatively high number of multilayers (- 30 to 60) should give a measurable resistance due to a film thickness of approximately 75 to 150 nm. In addition, no extraordinary increase in selectivity could be detected (apart from the two exceptions mentioned). It is, at present, very difficult to draw conclusions about changes in the process parameters from the experimental data. A number of additional experiments would be necessary for this purpose.

3.3.4. Gas separation measurements of PECVD- and 1=-PCVD-Si#N4 coated membranes

[n contrast to the LB-transfer, coating by PECVD and LPCVD strongly reduces the flow and permeability of the composite membrane. This k evidenced in figure 11 where the reduced permeabilities of PECVD- and LPCVD-coated membranes with and without intermediate layers are compared.

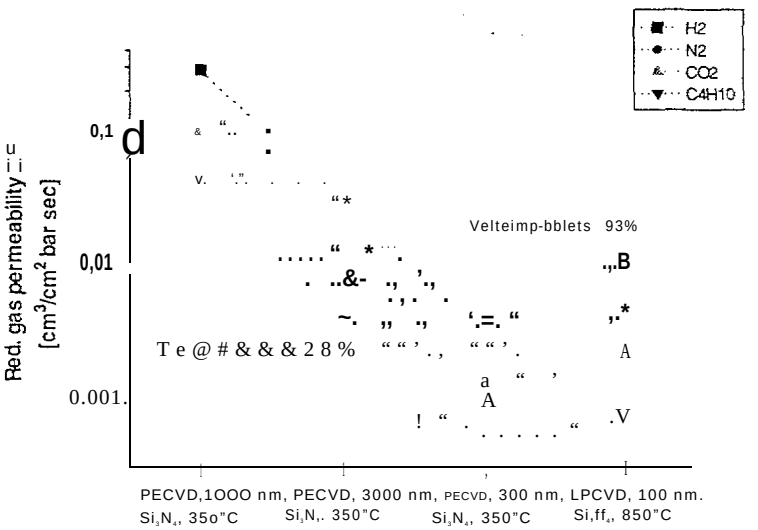

Fig. 11: Reduced permeabilities of PECVD- and LPCVD-Si_3N_4-membranes with and without inter mediate layer.

Although thick PECVD-films (1000 and 3000 nm) have been deposited on the membranes without intermediate layer, the reduction of flow relative to that of the uncoated suppo'ti is lower- compared to that of thin films (100 and 300 mm) on tablets

with intermediate layer. This is due to the' presence of the intermediate layer which reduces the pore size and surface roughness of the under[yktg SUppOrt. on modified supports of that kind selective layers can be deposited with a very limited number of defects, thereby allowing a very effective reduction of the flow. The permeabilities (layer thickness * reduced permeability) of these PECVD- and LPCVD-coated membranes are similar.

Although the reduced permeability is strongly influenced by the choice of the membrane and layer thickness (see figure 11), a difference in selectivity can only by found for the 100 nm LPCVD-membrane (see figure 12). [n particular, this tablet shows a high hydrogen/butane ratio (- 16).

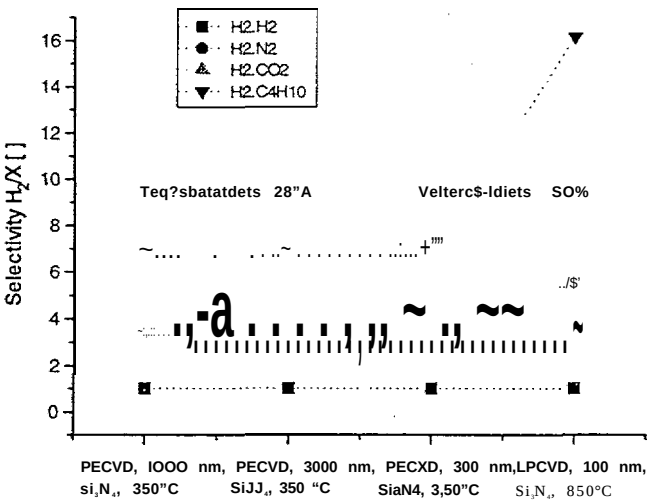

Fig. 12: Selectivities of PECVD- and LPCVD-Si_3N_4-membranes with and without intermediate layer.

As a second approach to increase the reduced permeability, the thickness of the deposited layer was decreased. Starting from Si_3N_4 films of 300 nm which were impermeable for any gas, the film thickness was reduced to 100 nm. These films, again, showed only very low gas permeabilities. Therefore, films were prepared having film thicknesses nearly in the range of conventional LB-muMilayers (74 and 50 rim). Their reduced permeabilities are shown in figure 13.

On the contrary to the expectations, the perrneabilities did not increase, but decreased considerably. The membranes seemed to be nearly dense, especially for the gases of high molecular weight, namely carbon dioxide and butane. Even for the 50 nm sample no significant increase was found. Similar observations have been made for the plasma polymerized samp[es. Here, only for a very low film thickness of 16 nm an increase in permeability could be observed.

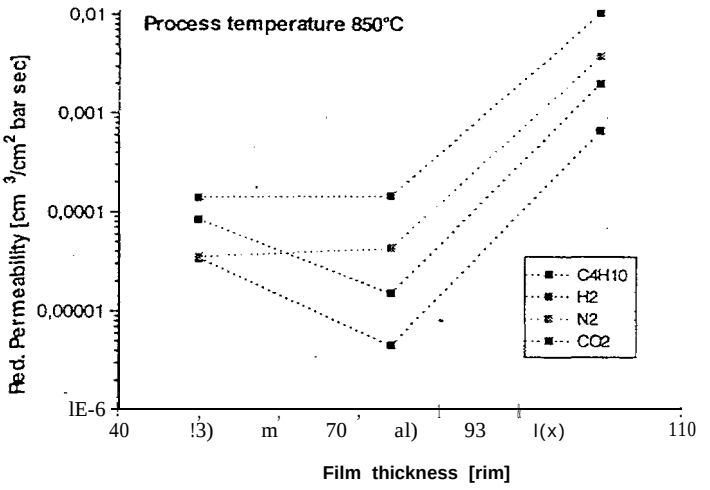

Fig. 13: Reduced permeabilities of LPCVD-Si_3N_4-membranes with intermediate iayer versus film thickness.

From these results the existence of two competing mechanisms cart be proposed: Firstly, a thicker film has a higher resistance compared to a thinner one due to the longer passage of the gas. At very low film thicknesses this effect is dominant which is evidenced by the significant increase in permeability. Secondly, a thicker film may contain more defects compared to a thinner film due to compatibility problems to the substrate, e.g. different thermal expansion coefficients. As a result of the competition of new flow regimes within defects with those of the defectfree volume (e.g. change from Knudsen to Pousei[le flow) the permeability as well as the selectivity is significantly altered. This second effect seems to be more dominant at higher film thicknesses.

The dependency of the selectivities on the film thickness is shown in figure 14.

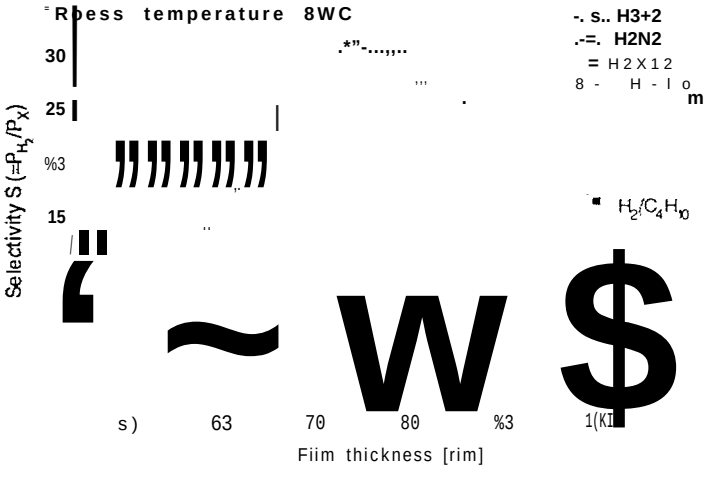

Fig. 14: Selectivities of LPCVD-Si_3N_4-membranes with intermediate layer versus film thickness.

The 74 rim-sample shows a high selectivity of 33 for the separation of hydrogen/butane. The other selectivities are also enhanced. However, it has to be mentioned that the permeabiiities used for the calculation of the selectivities are low and that small abso[ute variations in the permeability, thus, significantly will influence the selectivity. At a still lower film thicknesses of 50 nm a drastic reduction of selectivity is observed. Similar observations were made for the plasmapolymerized films. This decrease in selectivity. may be caused by an incomplete coveringl of the intermediate layer by the deposited selective layer.

3.3.5. Gas separation measurements of piasmapolymerized Si02 membranes

FYasmapolymerization of HMDSO leads to a mixed inorganic-organic material whose elemental composition can be approximately described by "$Si0_2$" (with a considerable carbon content). This residual carbon content can be further decreased by pyrolysis of this material (600"C, 1 h). Layers of similar elemental composition, but different morphology can be prepared from HMDSN/0_2 as precursor material. They have a residual nitrogen content and are generally softer materials compared to the hard layers from HMDSO. It was shown for this type of "$Si0_2$"-iayers on polymeric supports that the morphology depends significantly on the type of the plasma applied, namely radio frequency (RF) or microwave (PAW) plasma.
A comparison of the selectivities. of the two f-lMDSN/0_2 samples shows that deposition by microwave plasma gives layers of higher selectivities (but low perrneabiiities), again the hydrogetibutane ratio is comparatively high (- 34). .

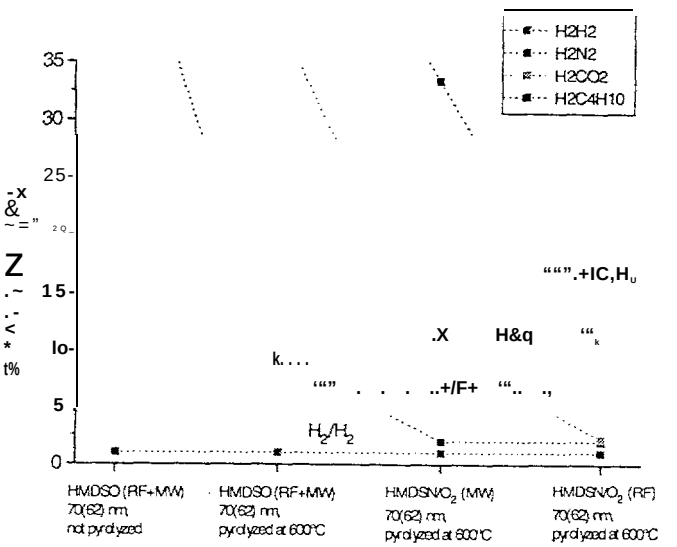

Fig. 15: Sefectivities of plasmapolymerized $Si0_2$ membranes with intermediate layer versus process parameters.

3.4. Performance of model calculations

3.4.1 Micropore size distributions from measured isotherms and grand canonical Monte-Carlo Simulations

Pores, and especially micropores (with sizes less than 2 rim), play an essential role in physical and chemical properties of industrially important materials like absorbents, catalysts, soils, biomaterials, etc. Their characterisation (in terms of pore size distribution and other structural information) is indispensable for the utilisation and design of improved porous systems in several applications. While for mesopores and macropores there exist a host of more or less established characterisation methods, the assessment of microporosity is much' less advanced despite the recent interest on microporous systems like zeolites, activated carbons and clay minerals [17]. The currently employed molecular (nitrogen) adsorption method is based on the thermodynamic approach of Dubinin who assumed that the micropore filling process is governed by a so called adsorption potential that characterises the adsorbed moiecules, and that the micropore size distribution is Gaussian. The Dubinin-Radushkevich (DR) equation relates the adsorbed amount per unit micropore volume to the temperature, relative pressure and the characteristic energy and affinity coefficients (which are in turn related to the isosteric heat of adsorption). The DR method has been subject to criticism mainly because the yety mechanism of molecular" adsorption in micropores is sti[l under active debate. [n fact, several studies employing both simulation and density functional theory have added to the accumulating evidence that none of the conventional adsorption methods of pore characterisation (such as Kelvin or DR analyses) is entirely satisfactory [18]. Improved approaches to the problem, based on mo!ecuiar level theories, should be developed.

The Monte Carlo technique has been found to be a promising tool in the study of adsorption of pure or multicomponent gases in zeolites and other micrcporous solids [19-24]. In this work, the method is used in its grand ensemble variant in combination with experimental isotherm data to characterise microporous structures and obtain the corresponding pore size distribution (PSD). Specifically, the mean C02 density inside a single slit shaped pore of given width is found on the basis of Grand Canonical Monte Carlo simulations for a predefine temperature and different relative pressures. Starting from an initial PSD guess, it is then possible to produce a computed C02 sorption isotherm and compare II to the measured one. After a few .-iterations, the procedure results in a PSD which, if desired, can be further refined at the cost of additional computational effort. Pore size distributions of membranes obtained by a Nitrogen porosimeter (with Krypton upgrade) via the conventional (DR) approach are employed for the sake of comparison with the present method.

3.4.2 Network model for the permeability of mesoporous media

In reference [25], **a detailed account of the rnodelling approach taken to simulate the transport process of permeate through the membrane is given. The basic elements of a network model are presented therein. The equations implemented for transport in each single pore of the network are presently applicable to pores larger than about 2 nrn in radius (mesopores) and involve Knudsen and Poiseuille gas flow, surface diffusion, condensate flow with meniscus enhancement and liquid Pojseuille flow. The ~orous structure is simulated bv a two-dimensional network of cylindrical pores**

with radii r following a given distribution function that can result from a measurement procedure or be selected among several possibilities (uniform, bimodal, skew triagonal, Gaussian, etc.). The pore connectivity is also variable. Depending on the specified pressure differential across the n&work, different flow regimes may develop inside the individual pores. As the effect of the network geometrical characteristics (pore size distribution, mean pore radius, pore connectivity) on condensable vapour permeability has been presented in the previous report, a further study on the influence of other significant parameters (surface flow resistivity, temperature, overall pressure drop across the membrane) is performed here. Reducing the medium resistivity to surface flow (expressed by the coefficient CR) by a factor of 3, affects significantly the permeability curve in the range of relative pressures before the occurrence and during the initial stages of capillary condensation. On the contrary, the part of the curve around the maximum remains practically uninfluenced due to the domination of the capillary mechanism there. H should be stressed again that the postulation for a constant coeticient of resistance to surface flow may not sound physically correct (a dependence on the degree of pore filling among others should be more realistic) but nevertheless it leads to safe qualitative predictions as far as the relative contributions of Knudsen, surface and condensate flow to the overaii permeation rate are concerned. The basic C_R vaiue used in the present simulations is an experimental finding from freon-113 transport through (mesoporous) Vycor glass., Rates of transport in ali flow regimes considered (Knudsen, surface, capiiiary enhancement, Poiseuiile) depend on temperature either straightforwardly or through the variation of physicai properties of the f!uid (mainly saturation pressure, viscosity and vapour density). The reduction in permeability is more pronounced in the capi[iary condensation regime despite the decrease of iiquid viscosity with temperature.

An extension of the code to three dimensions is currently underway permitting more reaiistic simulations. The current version features the possibility of seiecting any pore connectivity vaiue between 2 and 26 for the porous structure to be simuiated thus making the software quite flexible and permitting the comparison to actual experimental data. The initial (fuii, with diagonai connections) cubic structure of the nodes undergoes a reduction in connectivity by randomiy cutting pores untii the desired (prespecified) average vaiue is attained. The sizes of the remaining pores in the finai structure are then taking randomiy vaiues satisfying the given distribution function.

in addition to the above, a mathematically rigorous procedure has been established ieading to a reliabie criterion for the ioss of the menisci action (fiow enhancement) as the prevailing reiative pressure increases. it is shown that the meniscus fiattens out (infinite curvature, i.e. zero capiiiary pressure) as soon as the expected thickness of the adsorbed iayer (under the specific reiative pressure conditions) becomes equai to the radius of the pore. This result has been used on an empiricai basis (agreement with experiments) in previous studies.

The model wiil be used to study further the effect of pore shape (slits versus cylinders), pore constrictions, macroscopic inhomogeneities in pore size (to expiain observed differences in flow rates when the direction of flow is reversed) and dual porosity systems {fractured networks). Comparisons with experiments are aiso

performed fora rigorous testing of thespecific approach foliowed anda validation of the results obtained.

3.4.3 Relative permeability phenomena

The flow properties of porous media are reported to be extremely sensitive functions of the pore network structure. The most important flow property, for deriving significant information about the network structure, is considered to be the Relative Permeability (PR). [t is defined as the permeability of a fluid through a porous media, partially blocked by a second fluid, normalised by the permeability through the same porous solid, when the pore space is free of the second fluid 126].

Several studies have been presented 126-27] concerning relative permeability measurements, as well as calculations of the relative permeability model networks [28-29]. However and despite of its importance, the application of the method is not very wide, mainly due to two factors:

a) The experimental complications arising from the two component mixing requirements, ahd
b) The effect of macroscopic non-homogeneity. ‘

Relative permeability measurements are mainly presented in plots of P_R Vs, where Vs is the amount adsorbed by the solid at the relative pressure at which the relative permeability was measured. Of great significance are also relative permeability measurements made during resorption. Such measurements will be presented in this report.

3.4.4 Example of an experimental test

Two well-defined mesoporous Alumina porous pe[lets were involved in the following experimental procedure. They were made by symmetrical compaction of allumina powder consisting of eqtial spherical particles of 10 nm diameter. Special care was taken in order that macroscopic inhomogeneities to be avoided. Several sectors of the resulted pellets’ surface were tested by means of nitrogen adsorption isotherms in order to calculate the pore size distribution and verify that the pellets were microscopically defect-free.

Both membranes were simultaneously equilibrated with water vapour at several relative pressures. During equilibrium special care was taken so that, the membranes were not exposed, at any time, to a relative pressure higher than the one of the final equilibrium.

After equilibrium was reached, the low pressure sector of the testing rig was isolated from the high pressure one, and helium was inserted in the high pressure tank. Helium was mixed with the water vapour by means of a customised gas tiirculator for a time period of 12 hours. After the mixture reached a state of homogeneity , the first membrane was exposed and the helium permeability was measured. After completing the measurement for the first membrane, the low pressure sector was evacuated, and the proper amount of water was inserted, in order for the second membrane to be kept under proper equilibrium conditions. The measurement for the second membrane was ‘carried-out in the same fashion as the first one.

Fig. 1 Shows the PR V~ P/P. plot. It is obvious that at the same equilibrium conditions, the permeability of Membrane 2 (Higher Porosity) is proved to be slightly higher than the respective one of Membrane 1 (Lower Porosity). However, these differences are not very significant due to the very smali difference in the overaii porosities.

FIGURE 1

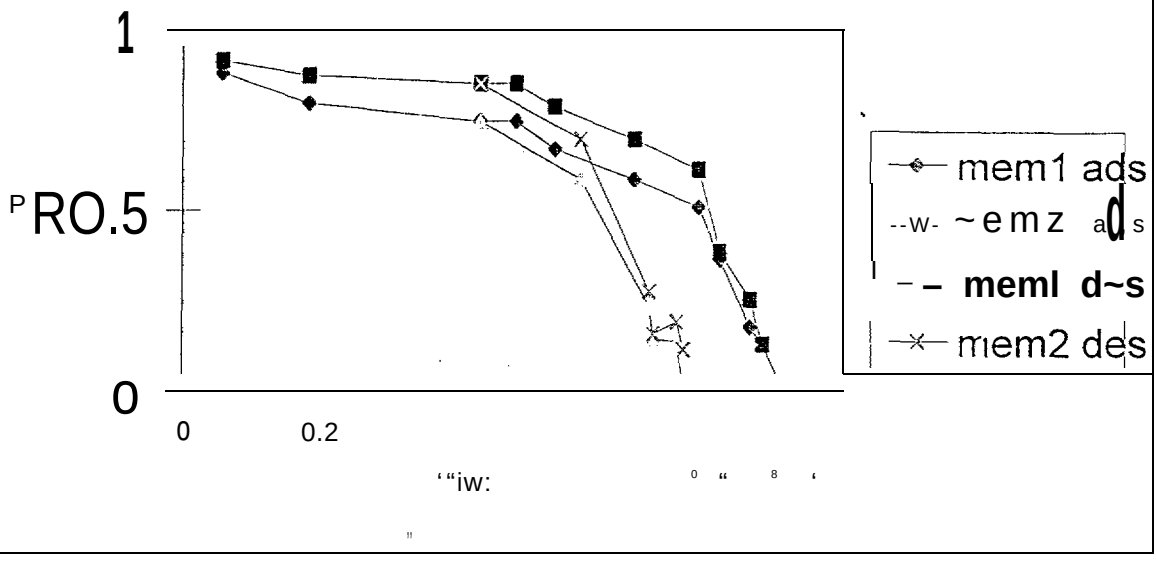

The He permeability diminishes at a reiative pressure of 0.85 for both membranes. This relative pressure corresponds to the percolation theshoid.

From the comparison of the PR of both membranes at the same reiative pressure during adsorption and resorption, it is observed that for reiative pressures higher than 0.6, PR is smaiier during resorption. This is due to the fact that within the hysteresis ioop of the isotherm of the mesoporous peiiet, the amount adsorbed is aiways greater during resorption than the one measured during adsorption for the same reiative pressure.

4. Summary

The project yielded a lot of highly interesting results from the technological as well as from the scientific point of view: Ultrathin films of high temperature stability and relatively homogeneous morphology have been prepared by a proper choice of the parameters of the plasma process. A deeper understanding of fundamental interactions between different kinds of plasma and a ultrathin LBlayer has been reached. Nevertheless, one of the main objectives, the preparation of an ultra-thin membrane film could not be reached, because it was di~icult to transfer these promising results to technologically relevant types of membranes. Here, not only the complex interactions caused by the plasma had to be controlled, but, in addition, it was realized that mariy of the supports available are not ideal for LB transfer. Thus, at present it seems that such plasma converted LB-films have more potential for applications which do not demand transfer on porous substrates of large area, but where deposition can be also performed on small dense ones. This is the case in sensor applications where usually only very small areas have. to be coated, so that the risk of cracks due to shrinkage and the defects is reduced substantially.

Furthermore, the hollow and flat ceramic membranes developed at TNO/CTK are already without additional coating of high interest for industrial applications in the field of ultrafiltration of liquids. The same is true for some of the silicon dioxide and silicon nitride intermediate layers produced by LPCVD and plasma polymerization which showed remarkable selectivities for hydrocarbons and hydrogen. Distinct dependencies between gas permeation and membrane properties e.g. layer thickness or process temperat~re, have been observed and can be used for a further tailoring of these membranes. Such layers are also highly mechanically chemically and thermally stabie and could be a starting point for further developments in the direction of high performance gas separation membranes.

5. Acknowledgements

We acknowledge the financial support of **the** European Union **which enabled us to ' run this focused fundamental research project.**
We also wish to thank the industrial endorsers, Dr. Ellinghorst (Deutsche Carbone, AG, Neunkirchen-Heinitz, Germany), Dr. Reichelt (AKZO Central Research, Obernburg, Germany), Mr Velterop (Velterop Membrane Technology, Enschede, The Netherlands), Mr. Travassaros (FOCO LTll -Solar Energy, Athens, Greece) and Mr. Soria (SCT Societe des Ceramiques Techniques, Bazet, France) for accompanying the project and for the stimulating discussions during the technical meetings.
Many thanks to our project officer from the European Commission, Dr. H. L. Schmidt, for his kind support in all technical and administrational questions concerning the work under the project.
Last but not least we as coordinator thank our partners from TNO/CTK in Eindhoven, the TNO in Delft and DEMOKRITOS in Athens for the fruitful cooperation in a friendly atmosphere and their kind hospitality during the project meetings.
S~ecial Thanks to our former coworker. Dr. A. A. Kalachev. on whose ideas the p;oject was based, for working out the proposal and bringing together the consortium during the first stage of the project.

6. References

(1) **G. Roberts in** *"Langmuir-B/odgeff Films",* **Plenum Press, ,New York, 1990**

(2) A. U I man, *"An Introduction to Ultrathin Organic Fiims. From Langmuir-B/odgeff fo Self- Assembty",* **Academic Press, Inc., San Diego, 1991**

(3) C. Naselli, J.P. Rabe, J.F. Rabolt, J.D. Swalen, *Thin Solid Films, f34* (1 *985) 3173*

(4) I.R. Peterson, J. Mol. *Hecffi,* **2(1986) 95**

(5) A. Barraud, J. Leioup, P. Maire, A. Ruaudel-Teixier, *Th~n Solid Films, 133(1985) 133*

(6) A.A. Kalachev, K. Mathauer, U. t-lohne, H. Mohwald, G. Wegner, *Thin Soljd Films, 228 (1 993) 307*

(7) P. Tippmann-Krayer, W. Meisel, H. Mohwald, Adv. *Mafer., 2(f* **2) (1990) 589**

(8) P. Tippmann-Krayer, R.M. Kenn, H. Mohwald, *Thin Solid Films, 2fO\2f 1 (1992) 577*

(9) P. Tippmzmn-Krayer, H. Mohwald, **M. Schreck, W. Gopel,** *Thin Solid Films, 213 (1 992)* 136

,(10) P. Tippmann-Krayer, W. Meisel, U, Hohne, H. Mohwald, *Makromol. Chem., Macromol. Symp.,* **46 (1991)24**

(11) **U. Hohne, t-l. Mohwald,** *Thin Solid Films, 243 (1994) 425*

(12) A.A. Kalachev; T.A. Klyushina, A.M. Shapiro, V.L. Kofman, S.D. Artamonova, N.A. Plate, *Polym. SC, U.S.S.R, 29 (1987) 202*

(13) A.A. Kalachev, G. Wegner, *Makromoi. Chem., Macromol. Symp., 46 (1 991)229*

(14) H. Kiessig, *Ann. Phys, 10 (1931) 769*

(15) J. D. Swalen, J. F. RaboH in *"Fourier Transform infrared Spectroscopy. Application to Chemiea{ Systems Vo/ume 4"* **edited by J. R. Ferraro and L.J. Basile, chapter 7, pages 283- 3?4, Academic Press (1985)**

(16) J.F. Rabolt, F.C. Burns, N.E. Schlotter, J.D. Swalen, J. Chem. Phys., 78(2) (1983) 946

[17] K. Kaneko, J. Membrane Sci., 96, 59-89 (1994)

[18] D, Nicholson, ,J. Chem. Sot. Faraday Trans., 90(1), 181-185 (1994)

[19] J.L. Sc)to et al., J. Chem. Sot. Faraday Trans. 1,77 (1981)

[20] F. Karavias and A. Myers, Mol. Sire., 8,51, (1591)

[21] D,M. Razmus and C.K. Hall, AIChE J., 37,5, (1991)

[22] R.F. Crackne[l et al., Mol. Phys., 80(4), 885 (1993)

[23] R.F. Cracknell et al., Mol. Sire., 13,161 (1994)

[24] R.F. CrackneU et al., J. Chem. Sot. Faraday Trans., 90(1 1), 1487 (1994)

[25] M. Kainourgiakis A, K. Stubos, N.K. Kanellopoulos. " A *Network Model for Vapow Adso@ion and Transport ;n Mesoporous Membranes"* **in press for the J:** *of Membr. Sci.*

[26] **N.K. Kanellopouios and J.H. Petropoulos Chern Sot.** *Faraday Trans. 1.198379517-525,*

[27] **T.A. Steriotis et. al.** *J. of Porous fvlateriats 2,73-751995*

[28] J.H. Petropoulos, J. K. Petrou, N.K. Kanellopoulos Chern Eng. Sci. 4429671989.

[29] N. **K. Kanellopoulos et. al. J.** *Of Co//oid. and hfreface Sci. 961983101:* **New** *apparatus for gas* **Abso/ute** *and* **Gas** *Relative Permeability Measurements in Porous Solids"* **in Press fort he** *Rev. of Sci. Instruments.*